THE WAKEFIELD, VIRGINIA WSR-88D DEPICTION OF THE 6 SEPTEMBER 1994 SPLIT CELL THUNDERSTORM OVER SOUTHERN VIRGINIA

Neil A. Stuart

National Weather Service Office
Wakefield, Virginia

Abstract

On 6 September 1994, an isolated thunderstorm over southern Virginia split into separate left-moving and right-moving thunderstorms with respect to the mean 0–6 km wind. The left-mover maintained its strength longer than the right-mover, and each storm produced large hail along their respective storm paths. An analysis of the structure of the thunderstorms was performed through an examination of products from the Weather Surveillance Radar-1988 Doppler located in Wakefield, Virginia. The structure of the thunderstorms, with respect to base reflectivity and internal wind structure, indicated characteristically high reflectivity returns, cyclonic rotation in the right-moving storm and anticyclonic rotation in the left-moving storm. However, the left- and right-moving storms also exhibited oppositely rotating regions within each respective thunderstorm, possibly induced by each storm's stronger dominant rotation. Also, low-level rotational velocities associated with the thunderstorms were indicative of possible tornadic activity yet tornadoes or funnel clouds were not observed. The absence of tornadic activity was most likely due to an unfavorable vertical wind profile in the storm-scale environment and the lack of depth of the circulations.

1. Introduction

Conceptual models of the characteristics of splitting thunderstorms were first developed over 35 years ago when Hitschfield (1960) observed splitting thunderstorms on radar near Montreal, Canada. However, analysis of their splitting cell storm structure through the use of Doppler radar observations has not been extensively documented.

The generally accepted conceptual model for splitting thunderstorms (such as Wilhelmson and Klemp 1981) describes cyclonic rotation in the right-moving storm and anticyclonic rotation in the left-moving storm. A recent study by Brown and Meitín (1994) described Doppler radar observations of dominant left-moving storms in North Dakota. Rotating updrafts were not observed within right-moving and left-moving storms. However, during the splitting process, cyclonic vertical vorticity was observed in the developing right-moving storm and anticyclonic vertical vorticity in the developing left-moving storm, which continued through the life of each storm.

This study documents the life cycle of a splitting thunderstorm, which occurred in southern Virginia on 6 September 1994, based on Doppler radar observations from the Wakefield, Virginia (KAKQ) Weather Surveillance Radar-1988 Doppler (WSR-88D). A single thunderstorm developed around 2200 UTC 6 September 1994 near Volens, Virginia in Halifax County. The storm began to move southeastward at approximately 20 kt and generally with the mean wind until about 2250 UTC, when the split occurred. The left-mover tracked nearly due east through Charlotte, Lunenburg, southern Nottoway, Dinwiddie and southern Prince George Counties. The right-mover tracked southeast through eastern Halifax County and Mecklenburg County, then dissipated as it entered North Carolina. Large hail was produced by both storms. However, tornadoes were not reported and only two events of minor wind damage were observed. The left-mover was the more dominant storm, maintaining its strength longer than the right mover.

The WSR-88D storm-relative velocity data indicated low-level velocity couplets within each storm. The right-mover exhibited cyclonic rotation on the southern (inflow) side, while the left-mover exhibited anticyclonic rotation on the southern side. Conversely, the rotation on the north sides of the right-moving storm and left-moving storm were anticyclonic and cyclonic, respectively. Interestingly, the strongest rotation observed in both storms was cyclonic. The low-level rotations suggested possible tornadic activity in both storms based on the magnitude of maximum inbound and outbound values observed by the WSR-88D (Kuhl 1994; Burgess et al. 1995), but tornadic activity was not observed. The lack of tornadic activity was possibly due to the unidirectional wind profile in the thunderstorms' environment, and the shallow nature of the internal circulations.

The WSR-88D radar products presented in this study will focus on the base reflectivity and storm-relative velocity characteristics of the splitting thunderstorm and the resultant left- and right-moving storms. Atmospheric soundings and hodographs generated by using the Skew-T Hodograph Analysis and Research Program (SHARP; Hart and Korotky 1991) workstation, will also be presented to illustrate atmospheric stability and vertical wind shear characteristics of the split cell thunderstorm environment.

2. Characteristics of Splitting Thunderstorms

Many cases of splitting thunderstorms have been documented. Burgess et al. (1976) focused on 16 splitting pairs and created a table of basic characteristics of splitting thunderstorms. Brown and Meitín (1994) updated the table to 31 pairs and summarized the characteristics based on this larger data set. They concluded that right-movers deviated an average of 29° from the mean wind (typically density or pressure-weighted mean from cloud base to the tropopause) at a speed of about 22 kt, while left-movers deviated an average of 26° at about 34 kt. The left-mover propagated faster than the right-mover in all 31 cases. Both storms can produce hail, but right-moving storms produced tornadoes more consistently than left-moving storms. Damaging winds are a less reported phenomena but are possibly overlooked due to the more noteworthy hail or tornado damage.

The evolution of splitting storms as depicted in radar reflectivity was described by Achtmeier (1969); Burgess et al. (1976);

and Brown and Meitín (1994). They proposed the following sequence of events:

1) Formation stage. The thunderstorm develops and begins to propagate while a pronounced reflectivity gradient develops along the thunderstorm's rear flank;

2) Elongation stage. The thunderstorm elongates into an elliptical shape with the major axis generally perpendicular to the direction of storm motion. The intense reflectivity core splits and each core grows apart as the reflectivity gradients intensify along the left and right storm flanks;

3) Splitting stage. The central portion of the echo rapidly diminishes in size and intensity leaving two separate thunderstorm cells; and,

4) Deviation stage. The left-mover moves left of the mean wind and increases in forward speed. Conversely, the right-mover moves right of the mean wind and decreases in forward speed. Horizontal distance between the split storms increases with time.

Characteristics of Doppler radar velocity signatures in splitting thunderstorms are not widely documented but typical characteristics were described by Brown and Meitín (1994) based upon previous studies (Burgess et al. 1976; Kubesh et al. 1988; Brown 1992). Typically, the updraft of a right-moving storm rotates cyclonically and the updraft in the left-moving storm rotates anticyclonically. Additionally, the left- and right-movers can develop rotations characteristic of mesocyclones, each producing severe weather such as large hail, damaging winds and sometimes tornadoes.

However, the rotation (or vorticity) associated with the thunderstorm updrafts in previous studies was not always strong enough to be classified as a mesocyclone. Nominal threshold values for classification as a mesocyclone are a function of radar resolution. The WSR-88D radar mesocyclone algorithm assesses counterclockwise circulations, which are vertically correlated and are symmetrical (Klazura and Imy 1993). Consequently, left-moving, anticyclonically rotating thunderstorms cannot be labeled as a mesocyclone by the WSR-88D. The vertically correlated circulations must be detected on at least two consecutive elevation angles.

Specific rotation (or vorticity) value thresholds for mesocyclone detection are not applied to the Doppler radar data. Mesocyclone detection is based on the magnitude of shear for a region within a thunderstorm and is then checked for vertical correlation and symmetry (Federal Meteorological Handbook 11, Part C 1991). The NEXRAD (NEXt generation RADar) Weather Service Forecast Office (NWSFO) in Norman, Oklahoma (OUN) developed subjective thresholds for mesocyclone classification based on their past experience with rotating thunderstorms (National Weather Service 1994). Additionally, some preliminary values of average rotation depicted by the WSR-88D, for the formation of tornadoes in the NWS Eastern Region, have been determined based on a study of 15 confirmed tornado cases (Kuhl 1994; Burgess et al 1995). Average rotational velocities for F0 and F1 tornadoes at 0.5° or 1.5° were as low as 20 kt at a distance of 26.5 and 72.7 miles respectively from the Radar Data Acquisition (RDA) site. This is characterized as borderline *minimal mesocyclone* criteria determined in Norman, Oklahoma. Average depths of the circulations in the east coast tornadic storms were 10,000 to 11,000 ft for F0 and F1 tornado events.

The Norman NWSFO defines both 2 nm and 5 nm diameter mesocyclones as having a minimum of 25 kt average rotation (adding the maximum inbound and outbound velocities in the mesocyclone core and dividing by 2) within 5 nm of the RDA. However, at a range of 125 nm from the RDA, the values decrease to 15 and 21 kt for 2 and 5 nm diameter mesocyclones respectively. Figure 1 depicts nomograms of threshold values for minimal to strong mesocyclones with respect to average rotational velocity, mesocyclone diameter and distance from the RDA, developed by the NOAA National Severe Storms Laboratory (NSSL). These are the only nomograms that aid in determination of the strength of a mesocyclone that have been developed. Hence, the nomograms are used as reference throughout the NWS and are gradually being adjusted by local offices. Additionally, these circulations must last a minimum of 10 minutes. Vorticity value thresholds for mesocyclones vary from $1 \times 10^{-2}\ s^{-1}$ near the radar to $5 \times 10^{-3}\ s^{-1}$ beyond 100 nm from the RDA (Vasiloff et al. 1993).

3. Atmospheric Stability and Vertical Wind Shear

Figure 2 depicts the 0000 UTC 7 September 1994 sounding plot from Greensboro, North Carolina (GSO). This sounding was taken approximately 55 miles from the point where the thunderstorms developed, near Volens, Virginia, and 2 hours after the storms developed (Fig. 3). Although this sounding is not, by definition, a proximate sounding (Brooks et al. 1994), it was the closest upper-air observation to the event. Observed

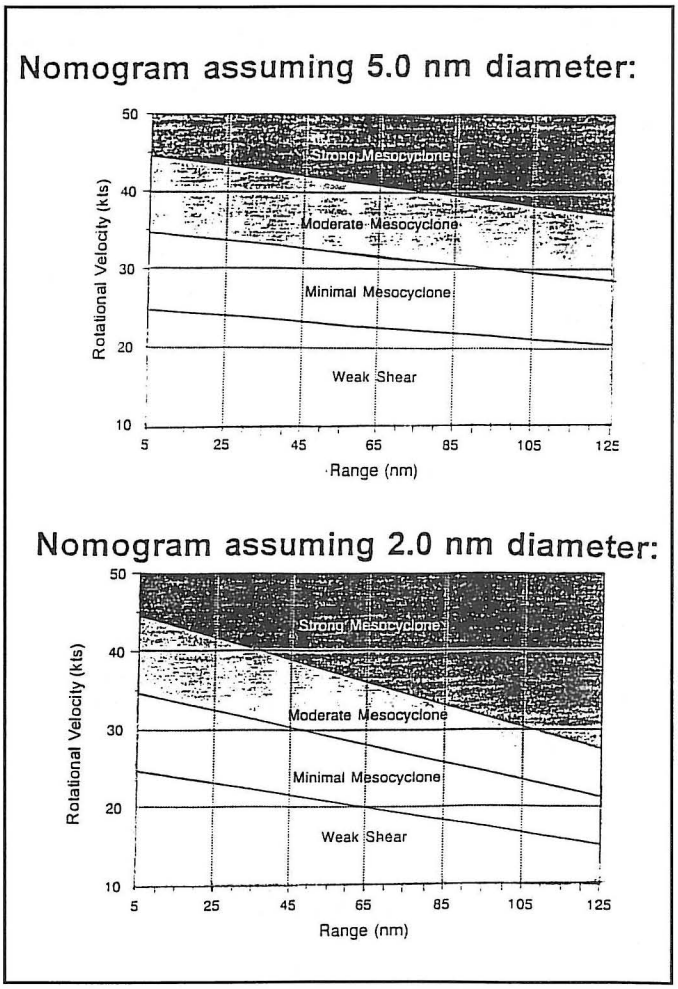

Fig. 1. The modified NSSL/WSFO OUN/OSF mesocyclone nomograms based on a mesocyclone diameter of 5.0 nm and 2.0 nm. From the OSF Operations Training Branch (National Weather Service 1994).

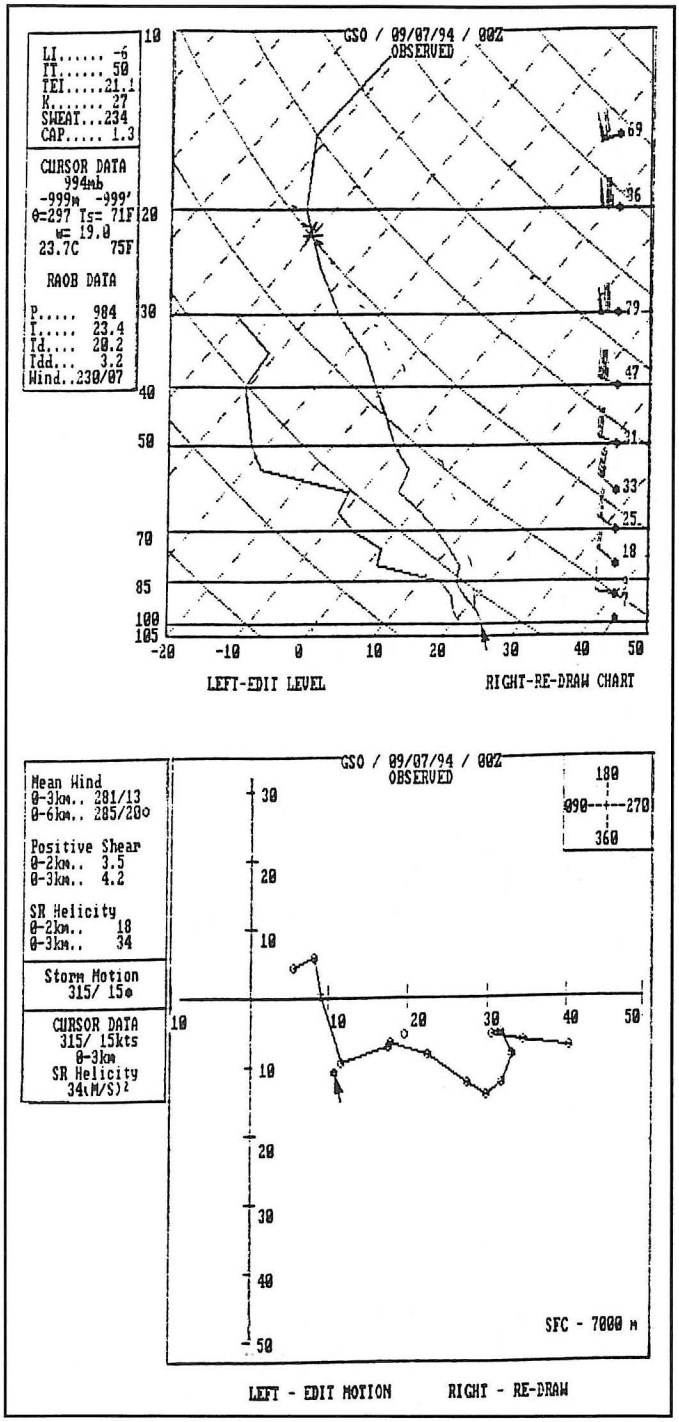

Fig. 2. The 0000 UTC 7 September 1994 Greensboro, North Carolina sounding and hodograph (From SHARP Workstation, Hart and Korotky 1991).

and modified sounding parameters from the 0000 UTC 7 September 1994 GSO sounding did support the development of split cell thunderstorms. Additionally, low-level flow was from the southwest and upper-level flow was uniform from the northwest. The vertical wind profile from the 0000 UTC 7 September GSO sounding was in close agreement with the Velocity Azimuth Display Wind Profile (VWP) from KAKQ. This implies that the wind profiles and advection patterns across southern

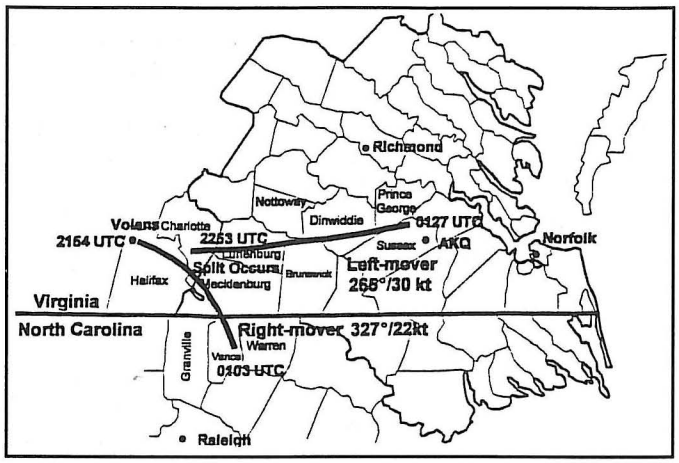

Fig. 3. Map of southern Virginia and northern North Carolina with the tracks of the splitting thunderstorms. Counties that are labeled were affected by the storms. The time of development of the initial storm (2154 UTC), time of the split (2253 UTC), and time of dissipation of each storm (0103 UTC for the right-mover and 0127 UTC for the left-mover) are depicted along with mean storm motion for each storm (327° at 22 kt for the right-mover and 265° at 30 kt for the left-mover).

Virginia and northern North Carolina were quite uniform, and were representative of the GSO 0000 UTC 7 September sounding. GSO was the closest upper-air site and due to the fact that split cells did occur, observed and modified GSO sounding parameters are considered to reasonably represent the storm-scale environment over southern Virginia.

Significant instability was present with a Lifted Index (LI) of −6 (surface based) and Convective Available Potential Energy (CAPE) of 1535 J kg^{-1}. Further inspection shows that the Total Totals (TT) was 50 and the K Index was 27. A TT of 50 indicated a moderate potential for severe thunderstorms (Miller 1972) and a K Index of 27 suggested enough moisture for possible thunderstorm development. The relatively high TT was due to moist air between the surface and 850 mb while the relatively low K Index indicates a lack of deep moisture. The cap strength of 1.3° C suggests that if the boundary layer temperature was raised 1.3° C, convection could be initiated.

Two other dimensionless parameters, the Bulk-Richardson Number (BRN; Weissman and Klemp 1982) and the experimental Energy Helicity Index (EHI; Johns et al. 1990), can help alert forecasters to potential severe weather, particularly with the development of severe thunderstorms. A BRN of 45 or below supports supercell thunderstorms, while a BRN above 45 supports multicell storms. An EHI greater than 1.00 indicates there is sufficient shear and CAPE available for tornadic development, while an EHI of less than 1 supports single or multicell thunderstorms. The 0000 UTC 7 September 1994 GSO sounding indicated a BRN of 42, supporting supercell storms. However, the EHI was 0.17, which does not typically support tornadoes (Brooks et al. 1994).

Figure 2 also depicts an unedited 0000 UTC 7 September GSO hodograph, representing a vertical wind profile that virtually matched the KAKQ vertical wind profile through the episode. Veering of the wind with height was evident in the lowest 3 km of the atmosphere, with little directional shear present above 3 km. The Storm-Relative Helicity (SRH) was 34 m^2 s^{-2} (units henceforth dropped) for the lowest 3 km. This value

was well below 150, which is the threshold for mesocyclone formation described by Davies-Jones et al. (1990).

Substantial vertical speed shear was present as the wind speed consistently increased with height. Hodographs, which depict very little directional shear but considerable speed shear, can illustrate conditions favorable for splitting thunderstorms (Rotunno and Klemp 1982). Speed shear typically creates a horizontal vortex of some magnitude, exhibiting vorticity of which there are two types, crosswise and streamwise, depending on the direction of low-level inflow (typically the 0–3 km layer).

Crosswise vorticity occurs when the low-level (0–3 km) storm inflow is relatively perpendicular to the horizontal vortex created by the speed shear. Conversely, streamwise vorticity occurs when the storm inflow is relatively parallel to the horizontal vortex created by the speed shear. The greater the streamwise vorticity, the more likely the thunderstorm updraft will begin to rotate and eventually develop into a mesocyclone. Predominant crosswise vorticity, however, will result in the updraft tilting the horizontal vortex differently, creating two oppositely rotating regions, cyclonic on the left side of the storm, with respect to the direction of the inflow, and anticyclonic on the right side. This can be a precursor to splitting thunderstorms and explains why the updrafts of right-movers and left-movers rotate cyclonically and anticyclonically, respectively. In this case, the mean wind direction of 285° resulted in a north/south oriented horizontal vortex.

The storm environment table calculated for GSO by the SHARP workstation for 0000 UTC 7 September, was based on a storm motion of 315° at 15 kt (SHARP produces the environment table based on a storm motion 30° to the right of the mean 0–6 km wind and 75% of the magnitude) and indicated relatively large values of horizontal vorticity but low values of streamwise vorticity in the lowest 3 km of the atmosphere. The storm-relative, low-level (0–3 km) inflow was generally from about 90°–120° for a storm moving with the 0–6 km mean wind (285° at 20 kt). As a storm moves right of the mean wind (gradually closer to 315° at 15 kt) the low-level inflow comes from about 170°.

Conceptually, when the storm first developed (before the split occurred), the storm-relative, low-level inflow was generally from the east and interacted with the north/south oriented horizontal vortex. Also, it can be deduced that the storm-relative inflow was nearly perpendicular to the horizontal vortex resulting in a greater magnitude of crosswise vorticity (10×10^{-3} s^{-1} for a mean 0–6 km wind of 285° at 20 kt) than streamwise vorticity (-1×10^{-3} s^{-1} for a mean wind of 285° at 20 kt). Consequently, the initial thunderstorm updraft tilted the horizontal vortex in such a manner as to create oppositely rotating elements which eventually split into the left- and right-moving storms.

The magnitude of the low-level inflow (in addition to SRH), may dictate whether a thunderstorm can acquire rotation (Lazarus and Droegemeier 1990). Rotating thunderstorms usually do not develop if the inflow is less than 20 kt. The mean low-level (0–3 km) inflow at GSO was 8 kt, which was well below the 20 kt threshold.

Although analyzing the environmental characteristics of a storm with a motion selected by the SHARP workstation is useful, a more accurate assessment of the storm's environment can be made by editing the storm motion to depict the actual storm movement of the right- and left-movers. The vertical wind profile from GSO was available only for the 0000 UTC 7 September sounding, but since the thunderstorms were moving toward KAKQ and the KAKQ vertical wind profile was unchanged, the vertical wind profile had likely remained very similar at GSO through the episode. It was determined through observation (the author worked the radar through the entire event) that the storm motion of the right-moving storm and left-moving storm were 327° at 22 kt and 265° at 30 kt respectively.

The storm environment table based on a storm movement of 327° at 22 kt was nearly the same as the table based on a storm motion of 315° at 20 kt. The SRH did increase to 70, but this is still well below the threshold of 150, stated by Davies-Jones et al. (1990), for mesocyclone formation. There was, however, a change in the mean storm inflow to 170° at 17 kt. Values for streamwise and overall horizontal vorticity for the right-mover were 5×10^{-3} s^{-1} and 9×10^{-3} s^{-1}, respectively. Therefore, it can be deduced that the magnitude of crosswise vorticity was about equal to the streamwise vorticity.

Therefore, the right-mover encountered more southerly inflow which interacted with the north/south oriented horizontal vortex created by the (285° mean wind induced) speed shear. This new interaction resulted in an increase in the streamwise vorticity from -1×10^{-3} s^{-1} to about 5×10^{-3} s^{-1} and a decrease in the crosswise vorticity from 10×10^{-3} s^{-1} to 5×10^{-3} s^{-1}. It can be inferred from SHARP workstation calculations, that the right-mover's updrafts began to encounter an environment with nearly equal degrees of crosswise and streamwise vorticity (about 5×10^{-3} s^{-1}) for both cells over southern Virginia around 0000 UTC (2245-0000 UTC) 7 September after the thunderstorm split occurred. The increase in streamwise vorticity should increase the probability of the formation of rotating thunderstorm updrafts. However, as stated previously, the magnitude of low-level inflow also helps determine the possibility for the development of rotating updrafts. Additionally, the right-mover's inflow was 17 kt, which is just below the 20 kt threshold determined by Lazarus and Droegemeier (1990).

The 265° at 30 kt movement of the left-moving storm created a very different storm-relative environment than that of the right-moving storm. The SRH for this storm was -111, which indicates that the magnitude of the negative helicity for the left-moving storm exceeded the magnitude of the positive helicity for the right-moving storm. Additionally, the magnitude of the SRH was closer to the threshold of 150 for mesocyclone formation as determined by Davies-Jones et al. (1990). This may suggest that environmental conditions were more favorable for supporting an anticyclonically rotating updraft within the left-moving thunderstorm than for a cyclonically rotating right-moving storm. Consequently, the storm-relative environmental conditions may partially explain why the left-mover was more persistent than the right-mover.

The mean low-level storm inflow between 0–3 km was from the east at an average of 20 kt, which according to Lazarus and Droegemeier (1990), supports the possible development of rotation in the storm. Values for streamwise vorticity averaged about -5×10^{-3} s^{-1}, while overall horizontal vorticity averaged about 9×10^{-3} s^{-1}. Therefore, it can be inferred that the left-mover interacted with considerably more crosswise vorticity than streamwise vorticity.

4. Doppler Radar Depicted Storm Evolution

a. Evolution of reflectivity-based thunderstorm characteristics

Figure 4 depicts a four-panel display of base reflectivity at the 0.5° elevation angle beginning at 2200 UTC 6 September (upper left) and ending at 2253 UTC (lower right). A single thunderstorm can be seen developing northwest of Volens in

Halifax County, Virginia (about 95 nm from KAKQ the 0.5° elevation angle was at approximately 11,000 ft) which began to move southeastward, generally with the mean wind. At 2253 UTC (lower right) the first indications that the storm was splitting can be seen. The storm elongated and a new high-reflectivity core began to develop just northeast of the initial thunderstorm.

Further inspection of the thunderstorm during the initial stage of splitting at 2253 UTC 6 September (Fig. 5), revealed two distinctive high-reflectivity cores aloft at the 1.5° and 2.4° elevation angles. In fact, the highest reflectivities in the initial storm (59–67 dBZ) were at or below the 1.5° elevation angle while the highest reflectivities in the new storm (50–55 dBZ) were at or above the 1.5° elevation angle. The reflectivity return of 67 dBZ at the 1.5° elevation angle in the initial storm suggests that hail could be in the storm. The observed freezing level from the 0000 UTC 7 September GSO sounding was approximately 10,000 ft and the beam height at 1.5° was approximately 17,000 ft, above the freezing level, suggesting the high reflectivity was due to a mixture of rain and ice (Atlas 1990).

The WSR-88D vertically integrated liquid (VIL) product, which is useful for inferring the presence of hail in thunderstorms, indicated a value of 40 kg m^{-2} (units henceforth dropped) at 2253 UTC 6 September (Fig. 6). Based on reports of hail during the event, a VIL of 50–55 was the threshold for severe hail (3/4 in. or dime-sized diameter or greater). At 2259 UTC, the VIL increased to 52 indicating that hail was still likely present in the initial storm (right-mover, henceforth), but real-time reports were needed to confirm that dime-sized hail occurred shortly after this VIL was indicated. The VIL in the new storm (left-mover, henceforth) had increased to 27.

The four-panel, 2304 UTC, 0.5°, 1.5°, 2.4° and 3.4° elevation angle, base reflectivity display (not shown) revealed that the two storms had completely split. Each thunderstorm exhibited high-reflectivity cores, both at the surface and aloft, although the right-mover had higher overall reflectivities below 1.5° with 63–65 dBZ.

The VIL in the left-moving storm increased to 37 as the storm-scale environmental interaction with the right-moving storm ceased while the VIL in the right-mover dropped to 44. This drop in VIL could be attributed to a decrease in the number of high reflectivity targets in the storm such as hail or large raindrops. Therefore, it can be inferred that any hail present in the storm was likely falling and perhaps reaching the ground. Marble- to dime-sized hail was observed in the town of Clover in Halifax County at this time, as well as a report of a tree and utility line being blown down. These would be the only severe weather reports associated with the right-moving storm.

At 2316 UTC, a four-panel of base reflectivity at 0.5°, 1.5°, 2.4° and 3.4° elevation angles (not shown) indicated the left-mover had accelerated and moved slightly north of east to the Charlotte/Lunenburg County border while the right-mover had begun to veer southeastward. The right-mover remained the strongest with values of 60–66 dBZ returns at or below the 1.5° elevation angle (about 16,000 ft). The left-moving storm, however, had strengthened considerably with reflectivities reaching 57–62 dBZ at or below the 1.5° elevation angle (about 13,000 ft).

Figure 7 depicts a KAKQ WSR-88D composite reflectivity (CR) product valid at 2322 UTC with the storm tracks overlaid. Maximum reflectivities at this time in both storms were around 64 dBZ, although, the right-mover had a larger area of high reflectivity returns. Note the curved shape of the 60–64 dBZ core in the right-mover. This feature may be due to the strengthening cyclonic rotation which will be discussed later. The ring shown just north of the right-mover indicates that uncorrelated shear was detected in the thunderstorm, which also will be discussed later.

Also note the forecast storm tracks and the attributes table at the top of Fig. 7. The storm track algorithm predicted the diverging tracks of the storms, but as will be seen later, the actual storm tracks of the left-mover (265° at 30 kt) and right-mover (327° at 22 kt) were slightly more left and right than the predicted tracks (271° at 25 kt and 319° at 16 kt, respectively).

By 2328 UTC, the VIL in the right-mover dropped to 42 but the VIL in the left-mover increased to 53, which was the same VIL value reached by the right-mover when it produced dime-sized hail at around 2300 UTC. Dime-sized hail was observed in Victoria in Lunenburg County at around 2330 UTC, associated with the left-mover.

Figure 8 depicts a four-panel chronology of the base reflectivity products at the 0.5° elevation angle beginning at 2316 UTC. The 2334 UTC 0.5° elevation angle (upper right) base reflectivity display indicated 60–61 dBZ in both storms.

The right-mover maintained itself, continuing to show VILs in the 45–50 range through 2346 UTC. A four-panel display of base reflectivity valid at 2346 UTC (not shown) indicated 59–65 dBZ at or below the 1.5° elevation angle in the right-mover. However, the overall depths of the high-reflectivity cores in both storms were about equal with 52+ dBZ at or above 2.4° in the right-mover and at or above 3.4° in the left-mover.

A composite reflectivity product valid at 2346 UTC overlaid with the storm track and attribute table (not shown) also revealed that the right-mover was stronger at this time. The WSR-88D hail algorithm calculated a positive indication of hail in the right mover, but there was no indication of hail in the left-mover. Additionally, the radar adjusted the storm track forecast (323° at 22 kt in the right-mover and 270° at 24 kt in the left-mover) with movement of the storms being more divergent. Between 2345 UTC 6 September and 0000 UTC 7 September, the right-mover produced pea-sized hail from Boydton to the John Kerr Dam in Mecklenburg County.

By 2352 UTC 6 September, base reflectivity values at the 0.5° elevation angle in both storms dropped to 55–59 dBZ although the VIL in the left-mover increased to about 47 and decreased in the right-mover to about 37. At this time, the areal coverage of the left-mover began to decrease, possibly due to the narrowing of the radar beam closer to the RDA.

Figure 9 depicts a four-panel display of VIL products beginning at 0004 UTC 7 September and ending at 0022 UTC. During this time, the VIL in the right-mover increased for the last time, to 46, before beginning the process of steadily weakening. The right-mover was crossing the North Carolina/Virginia border into Vance County where the thunderstorm eventually dissipated.

The VIL in the left-mover increased to about 42 which may seem non-severe compared to the threshold of VILs in the lower 50s established earlier. However, the change in the volume sampling performed by the WSR-88D may change the representation of VILs. A fast-moving storm (such as 30 kt observed in the left-mover) may not be completely sampled, since the 9 elevation angle scan strategy used by the radar (Volume Coverage Pattern 21) can result in lower VIL estimates (Federal Meteorological Handbook 11, Part C 1991). Also, closer proximity to the RDA can result in anomalous VIL values. Therefore, the lower VIL estimates in the left-mover must not be misinterpreted as characteristic of a lack of presence of hail. VILs in both storms remained around 40 through 0022 UTC and continued to exhibit similar values until the storms dissipated.

A four-panel display of base reflectivity at the 0.5° elevation angle beginning at 0016 UTC 7 September and ending at 0033 UTC (not shown) indicated that the low-level base reflectivities in both storms slowly decreased from around 58 dBZ to 56 dBZ between 0016 UTC and 0033 UTC in both storms.

At 0039 UTC, a CR product (not shown) indicated 62 dBZ in the left-mover while the right-mover continued to weaken. Penny-sized hail was observed in McKenney in Dinwiddie County at around 0030 UTC. This supports the theory that lower VILs (of around 40, described earlier) still represented hail, and in fact, the size reached severe criteria.

b. Evolution of velocity-based thunderstorm characteristics

Prior to the split of the cells (between 2247 and 2253 UTC 6 September), there was no discernible velocity circulations observed on the 0.5° elevation angle storm relative velocity map (SRM) product (Klazura and Imy 1993). Unfortunately, at the time of the split, range-folding contaminated the display of the 0.5° elevation angle SRM product, especially with regard to the developing right-mover. Therefore, no specific conclusions can be made with regard to velocity signatures prior to the split. However, after the split occurred (approximately 2253 UTC), some discernible features developed in both the left- and right-moving storms.

Figure 10 shows a four-panel display of the 0.5° elevation angle SRM for the left-mover, beginning at 2259 UTC (upper left) and ending at 2316 UTC (lower right), while the right-mover was still contaminated by range-folding. However, the left-mover revealed inbound velocities of 16 kt on the west side of the storm. The inbound velocity feature persisted throughout the lifetime of the left-mover and was nearly always on the western edge of the main core of high reflectivities. The outbound velocities of 7 to 16 kt south and north of the inbound velocities infer anticyclonic and cyclonic rotation, respectively. Therefore, it can be inferred that there were cyclonic and anticyclonic rotations, which persisted in the left-mover. The inbound and outbound velocities remained relatively weak through 2316 UTC with maximum mean rotational velocity of 21 kt (16 kt inbound and 26 kt outbound).

Beginning at 2328 UTC, the primary velocity couplet of the right-mover was completely outside the area affected by range folding. Figure 11 depicts a four-panel display of the 0.5° elevation angle SRM beginning at 2328 UTC (upper left) and ending at 2346 UTC (lower right). The initial development of a significant low-level (0.5° or 9,000 ft) cyclonic rotation can be seen on the southern periphery of the right-mover at 2328 UTC with a mean rotational velocity of 21 kt (16 kt inbound and 26 kt outbound). This velocity couplet strengthened to a 35 kt mean rotational velocity (35 kt inbound and outbound) by 2334 UTC and persisted through 2340 UTC (45 kt inbound and 26 kt outbound). The rotation began to weaken at 2346 UTC to a 31 kt mean rotational velocity (36 kt inbound and 26 kt outbound).

The anticyclonic and cyclonic rotations within the left-mover were not as strong, averaging 16 kt for both cyclonic and anticyclonic. However, the inbound velocity on the western side of the high-reflectivity core was persistent. The cyclonic rotation on the north side of the storm strengthened to 26 kt for both the inbound and outbound velocities from 2334 to 2340 UTC. The cyclonic rotation then weakened to 7 kt inbound and 16 kt outbound. The outbound component in the anticyclonic rotation for the left-mover never exceeded 16 kt.

The mean cyclonic rotational velocity peaked at 35 kt in the right-mover and 26 kt in the left-mover at the 0.5° elevation angle, implying the possibility of tornadic activity in both storms (Kuhl 1994). However, even though some circulation was present at 1.5° elevation (not shown) in each storm, the centers of the circulations were not vertically correlated. Perhaps the circulation in the right-mover at the 1.5° elevation angle depicted maximum inbound and outbound values whose distance was too far apart to be classified as having enough shear to have a correlated circulation with the 0.5° rotation. The 1.5° circulation in the left-mover, however, was displaced slightly south (on the order of about 5 nm) of the 0.5° elevation angle circulation. The displacement in the left-mover and weak circulation in the right-mover at 1.5°, was supported by the fact that the radar did not correlate the circulations at 0.5° and 1.5° in both storms and did not detect mesocyclones in either storm. The high-reflectivity core of the right-mover described earlier, had a slight curvature. This was possibly due to the low-level circulations in the right-mover. The cyclonic rotation on the south side and anticyclonic rotation on the north side created a weak, broad inflow notch, even though the primary inflow was southerly as described in the atmospheric stability and wind shear section of this study. Additionally, the cyclonic rotation in the left-mover was on the northern edge of the primary downdraft, where the high-reflectivity core was. Therefore, some circulation could have reached the ground, aided by the thunderstorm downdraft, but no tornadoes or significant wind damage were reported.

A four-panel display of SRM at the 0.5° elevation angle beginning at 2358 UTC 6 September and ending 0022 UTC 7 September (not shown) indicated that the right-mover continued to exhibit a 35 kt mean rotational velocity, but steadily weakened afterward as it entered North Carolina. The left-mover, however, continued to exhibit inbound velocities on the west side of the high-reflectivity core through 0022 UTC, until the storm dissipated around 0130 UTC. Maximum inbound velocities never exceeded 16 kt, inferring that there was not significant rotation that could produce tornadic development (Kuhl 1994; Burgess et al. 1995). The anticyclonic and cyclonic rotation on the south and north sides, although weak, continued until the storm dissipated at around 0130 UTC.

5. Concluding Discussion

a. Summary of the storm-scale environment for the splitting thunderstorm

During the late afternoon and evening of 6 September 1994, an isolated thunderstorm developed over southern Virginia and split into left- and right-movers. The base reflectivity and storm relative velocity characteristics of the thunderstorms were analyzed by using products from the NWS Wakefield, Virginia, WSR-88D.

The pre-storm environment was analyzed by using the SHARP workstation. The results of this study indicate that there was sufficient instability and moisture to initiate and sustain convection based on the 0000 UTC 7 September GSO sounding, which, based on a close similarity of the vertical wind profile from the KAKQ VWP, may have been representative of the conditions at the time and location of the splitting storm.

The environmental vertical wind profile exhibited very little directional shear (southwest winds veering to northwest within the lowest 8,000 ft) but considerable speed shear (10 to 20 kt within the lowest 8,000 ft and 25 to 50 kt between 8,000 and 18,000 ft. The (0–3 km) helicity calculated for the right-mover was 70, while a value of -111 was calculated for the left-mover. These helicity values were below the threshold of 150

for mesocyclone formation stated in a study by Davies-Jones et al. (1990).

Also, the magnitude of the low-level (0–3 km) inflow for the left- and right-mover were 20 and 17 kt respectively, at or near the threshold for development of rotation (Lazarus and Droegemeier 1990). Consequently, rotation developed in both storms.

The possible catalyst for initiating the thunderstorm to split was the storm's interaction with a comparatively larger magnitude of crosswise vorticity than streamwise vorticity. Before the split, when the storm was generally moving with the mean wind, the inflow was from the east and interacted with the north-south oriented horizontal vortex created by the mean wind, increasing in magnitude with height, blowing from 285°. The thunderstorm updraft tilted the horizontal vortex and consequently, created oppositely rotating regions which initiated the split into left- and right-movers.

Both the left- and right-mover produced large hail and only two minor wind damage events were associated with the split storms. No tornadoes or severe wind damage were reported during the episode.

b. Conclusions based on radar evaluation

Products such as R, CR and VIL are effective when evaluating thunderstorms for the presence of hail. During this episode, low-level (the 0.5° elevation angle) reflectivities were generally at or above 58 dBZ when hail (severe or non-severe) was reported reaching the ground. It is useful to note the VIL value associated with the reported size of hail for later reference. Often, during any particular episode, an established VIL value will produce hail of the size that was produced previously for that VIL value. During this episode, the VIL value associated with severe hail was 50–55. The hail usually reaches the ground when the VIL decreases rapidly (1 or 2 volume scans or 6–12 minutes in Volume Coverage Pattern 21) due to the large-sized (often water coated ice) scatterers exiting the thunderstorm.

The SRM product is very useful for observing the internal wind structure within thunderstorms. Rotation can be detected in a thunderstorm before it becomes a mesocyclone by comparing inbound and outbound wind maxima for different elevation angles within the storm. It is also necessary to determine the distance between inbound and outbound wind maxima to evaluate the areal size of the rotation. The areal size of the rotation is important for determining the magnitude of azimuthal shear within the storm and whether it should or should not be classified as a mesocyclone. It is also important in determining whether only the thunderstorm is rotating, or if a tornado may be being produced by the rotating storm.

During the episode, the left- and right-mover exhibited different characteristics with respect to rotation. Due to range-folding, no definitive conclusions could be made with respect to wind structure prior to the split or when the split actually took place, but after the split, the internal wind structure for each storm was well depicted. The SRM products were closely scrutinized and some conclusions were made.

After the initial storm split into a left- and right-mover, the paths deviated from the 0–6 km mean wind of 285° at 20 kt significantly. The left-mover tracked from 265° at 30 kt which resulted in a 20° directional deviation from the mean wind. The right-mover tracked from 327° at 22 kt which resulted in a 42° directional deviation from the mean wind.

The right-mover developed a low-level (the 0.5° elevation angle) cyclonic rotation in the southern region of the storm within 30 minutes after the split occurred. The maximum low-level rotation occurred between 2334 and 2358 UTC 6 September, 45–75 minutes after the split occurred, with a peak magnitude of 35 kt mean rotational velocity. Rotation observed at the 1.5° elevation angle in the right-mover may have been characterized by shear too weak to be classified as a circulation linked with the rotation at the 0.5° elevation angle, due to the distance between the maximum inbound and outbound values (relating to symmetry) at the 1.5° elevation angle. The non-correlation of the circulations at the 0.5° and 1.5° elevation angles resulted in the radar not classifying the storm as a mesocyclone. The non-correlated circulations also resulted in a very shallow low-level circulation which could not strengthen enough to produce tornadic activity.

The cyclonic and anticyclonic circulations in the right-mover created a secondary inflow region on the east side of the storm. The secondary inflow created a broad region of low reflectivities or inflow notch, resulting in a high-reflectivity core exhibiting curvature. The primary inflow was southerly, described previously in the atmospheric stability and wind shear section and the evolution of reflectivity section.

The right-mover also exhibited a weak low-level anticyclonic rotation on the northern region of the thunderstorm. The peak mean rotational velocity for the anticyclonic rotation was 22 kt (outbound maximum of 26 kt was associated with the cyclonic circulation). This anticyclonic circulation was determined by observing the persistent inbound low-level signature on the north side of the high-reflectivity core. This may have been mostly in response to the relatively stronger cyclonic rotation to the south inducing an anticyclonic circulation to the north.

With the cyclonic/anticyclonic rotation signature in the right-mover (which was the initial storm before the split), the possibility existed that it was due to the storm trying to split again. The assertion that the right-mover was the initial storm before the split, can be made based on its maintaining its high reflectivity core during and after the split, while the left-mover developed its high reflectivity core only when the environmental interaction with the right-mover ceased. However, the tendency for the right-mover to split again was greatly reduced due to the primary low-level 0–3 km inflow from the south, increasing the magnitude of the streamwise vorticity and decreasing the magnitude of the crosswise vorticity. Therefore, the anticyclonic circulation was likely induced by the relatively strong cyclonic circulation rather than the right-mover's updraft interacting with crosswise vorticity creating oppositely rotating regions.

The left-mover retained its high-reflectivity core and produced severe weather longer than the right-mover. The greater persistence of the left-mover may be partially attributed to the relatively high magnitude of negative helicity compared to the positive helicity exhibited by the right-mover. Although neither thunderstorm developed into a mesocyclone, each did exhibit rotation, mainly at low levels (the 0.5° elevation angle). The SRH for the left-mover suggests that there was more support for mesocyclonic development for an already anticyclonically rotating thunderstorm, which possibly contributed to the greater persistence of the left-mover.

The anticyclonic rotation in the left-mover never exceeded 22 kt mean rotational velocity and often was only 16 kt. Therefore, the SRH was only a partial factor in the persistence of the left-mover. Other possible factors, such as propagation of the left-mover into an area with greater instability than the right-mover, could not be assessed. Vertical temperature and moisture profiles are not available for interior southeastern Virginia to assess parameters conducive for sustaining convection so no definitive conclusion can be made.

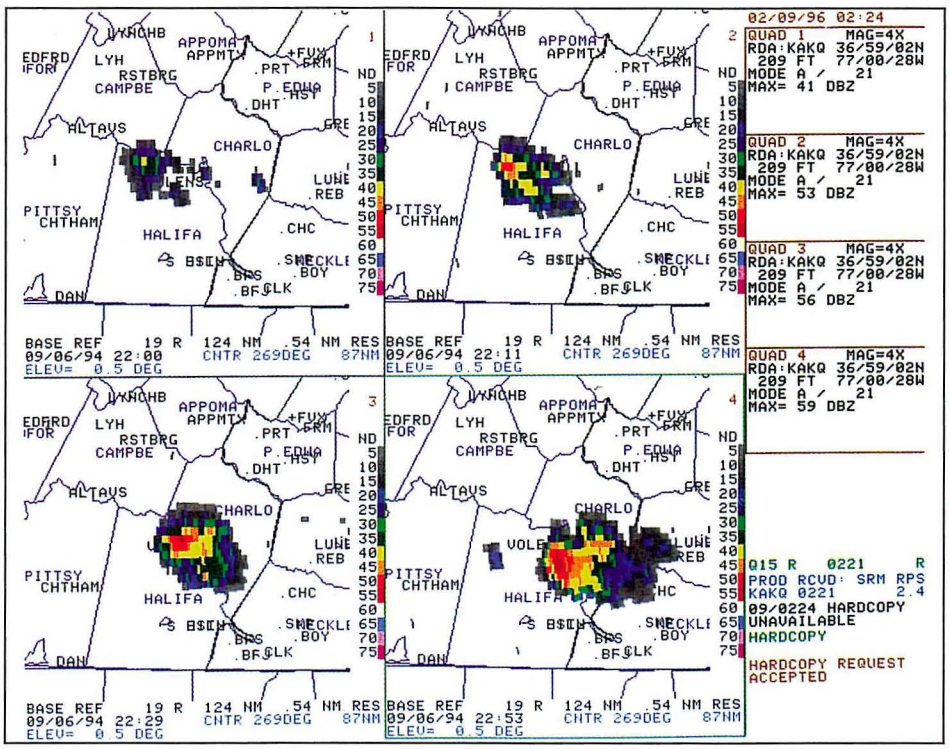

Fig. 4. The Wakefield, Virginia, WSR-88D four-panel base reflectivity product beginning at 2200 UTC 6 September 1994 (upper left) and ending at 2253 UTC (lower right). The color tables on the right of each quarter panel depict the intervals of reflectivity in units of dBZ. The elevation angle is 0.5°, range coverage is 124 nm (230 km) magnified two times, and resolution is 1° × 0.54 nm. Maps displayed are county boundaries and cities. The maximum reflectivity for each quadrant is listed to the right of the displayed products. Maximum reflectivities for each volume scan are 41 dBZ, 53 dBZ, 56 dBZ and 59 dBZ for quadrants one, two, three and four, respectively.

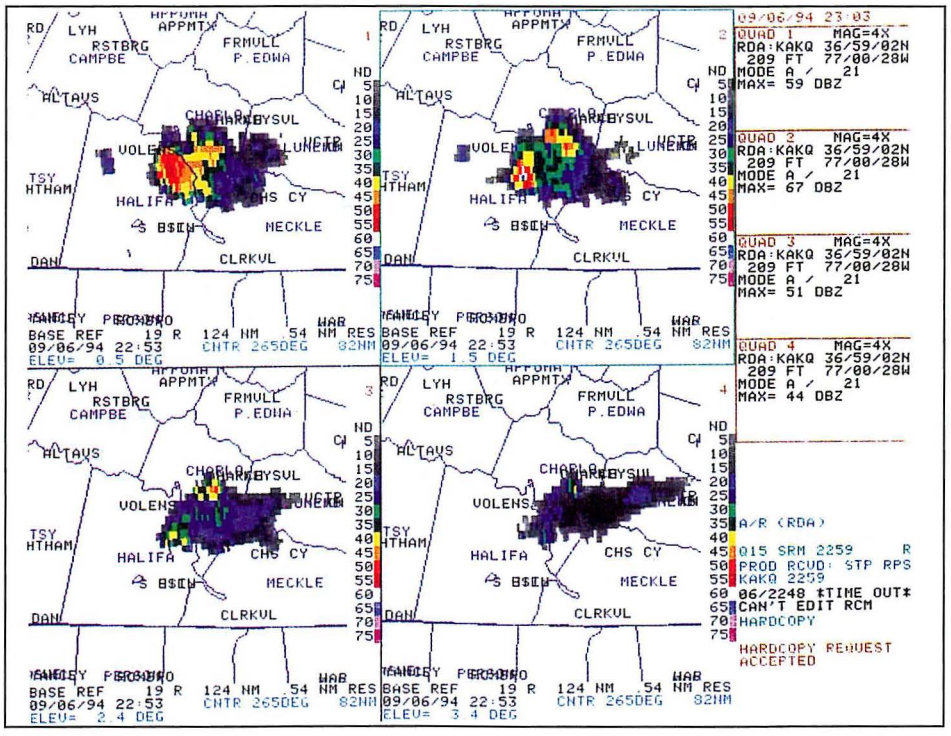

Fig. 5. The Wakefield, Virginia, WSR-88D four-panel base reflectivity product from 2253 UTC 6 September 1994 for the 0.5° (upper left), 1.5° (upper right), 2.4° (lower left) and 3.4° (lower right) elevation angles. The color tables on the right of each quarter panel depict the intervals of reflectivity in units of dBZ. The range coverage is 124 nm (230 km) magnified two times, and resolution is 1° × 0.54 nm. The maximum reflectivity for each quadrant is listed to the right of the displayed products. Maximum reflectivities for each volume scan are 59 dBZ, 67 dBZ, 51 dBZ and 44 dBZ for quadrants one, two, three and four, respectively.

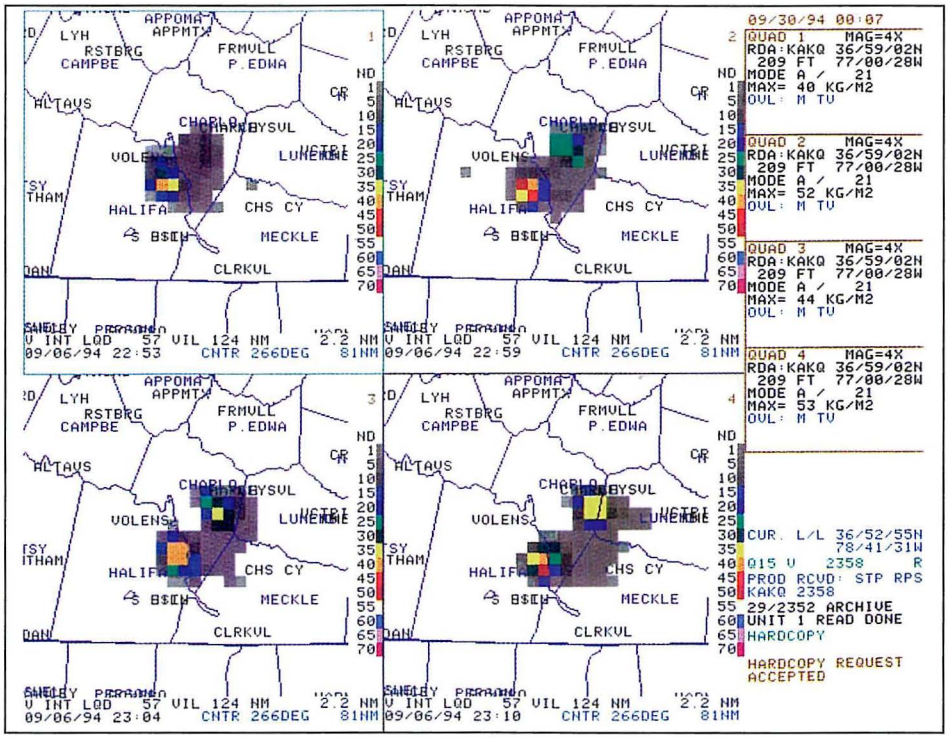

Fig. 6. The Wakefield, Virginia, WSR-88D four-panel vertically integrated liquid product beginning at 2253 UTC 6 September 1994 (upper left). The color tables on the right of each quarter panel depict the intervals of integrated amount of liquid in units of (kg m^{-2}). The range coverage is 124 nm (230 km) magnified two times, and resolution is 1° × 2.2 nm. The maximum vertically integrated liquid for each quadrant is listed to the right of the displayed products. Maximum values of vertically integrated liquid for each volume scan are 40, 52, 44 and 53 for quadrants one, two, three and four, respectively.

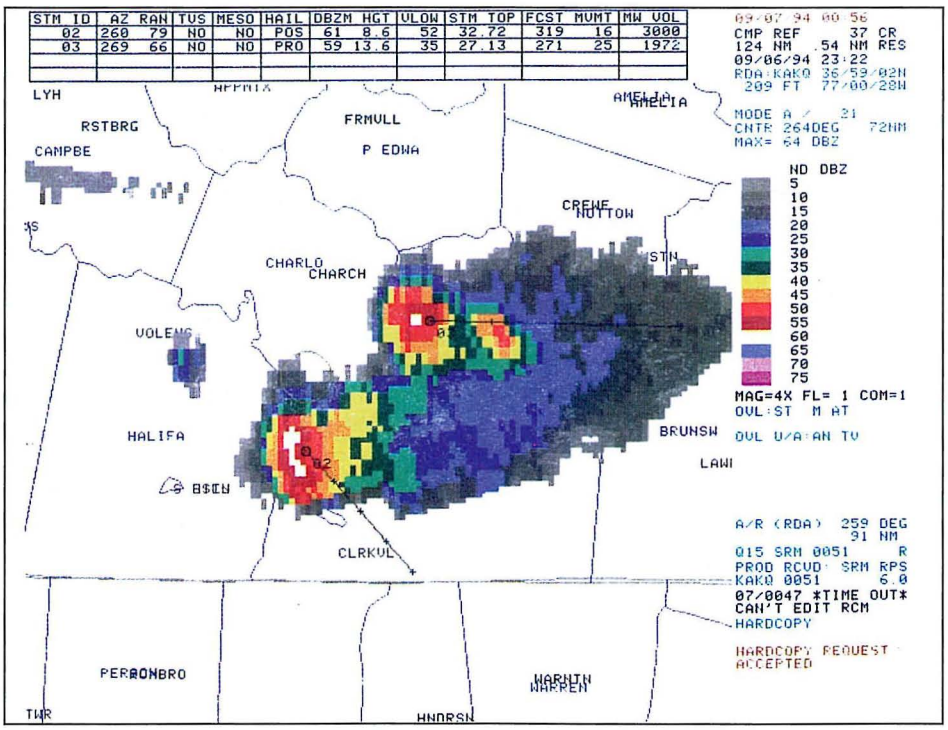

Fig. 7. The Wakefield, Virginia, WSR-88D composite reflectivity products at 2322 UTC 6 September 1994. The color tables on the right depict the intervals of reflectivity in units of dBZ. Resolution is 0.54 nm × 0.54 nm and magnified two times. Product overlays are mesocyclone, hail index, and storm tracking information associated with storms 02 and 03. Storm attribute table is located on top, which shows information on two storms (storms 02 and 03). The table shows azimuth(deg)/Range(nm) of the storm centroid (relative to the radar), whether a tornadic vortex signature, mesocyclone, or hail have been indicated, the maximum reflectivity (dBZ) and height (K ft) of the maximum reflectivity, maximum mean radial velocity detected at the lowest height sampled within the storm (kt), storm-top height (K ft), forecast direction (deg from which storm is moving) and speed (kt), and mass (Kg).

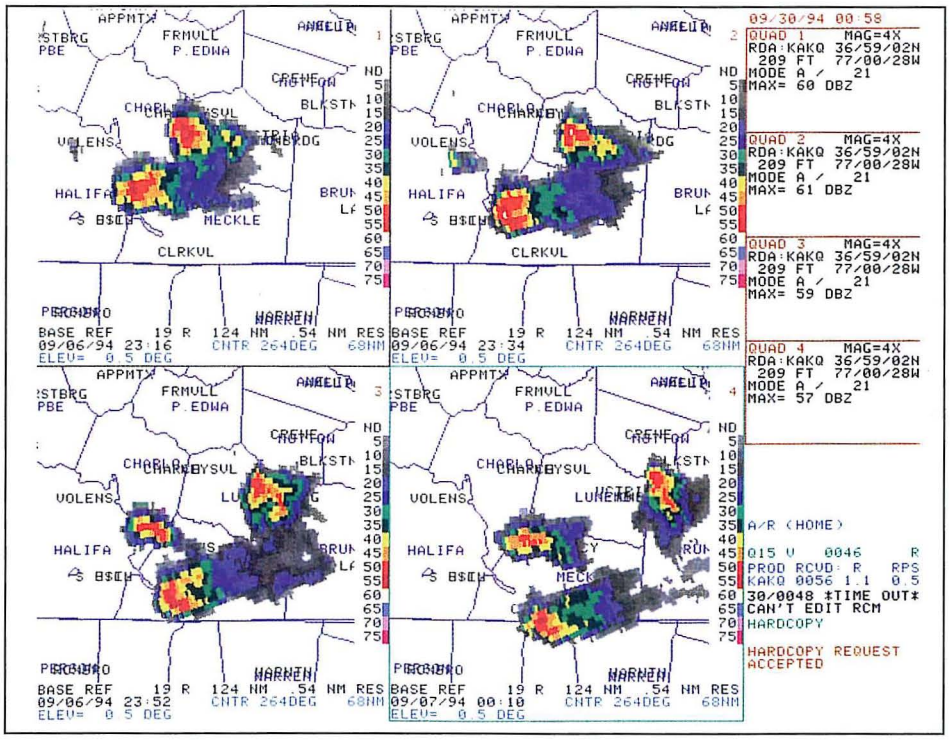

Fig. 8. Same as Fig. 4 except beginning at 2316 UTC 6 September 1994 (upper left). Maximum reflectivities for each volume scan are 60 dBZ, 61 dBZ, 59 dBZ and 57 dBZ for quadrants one, two, three and four, respectively.

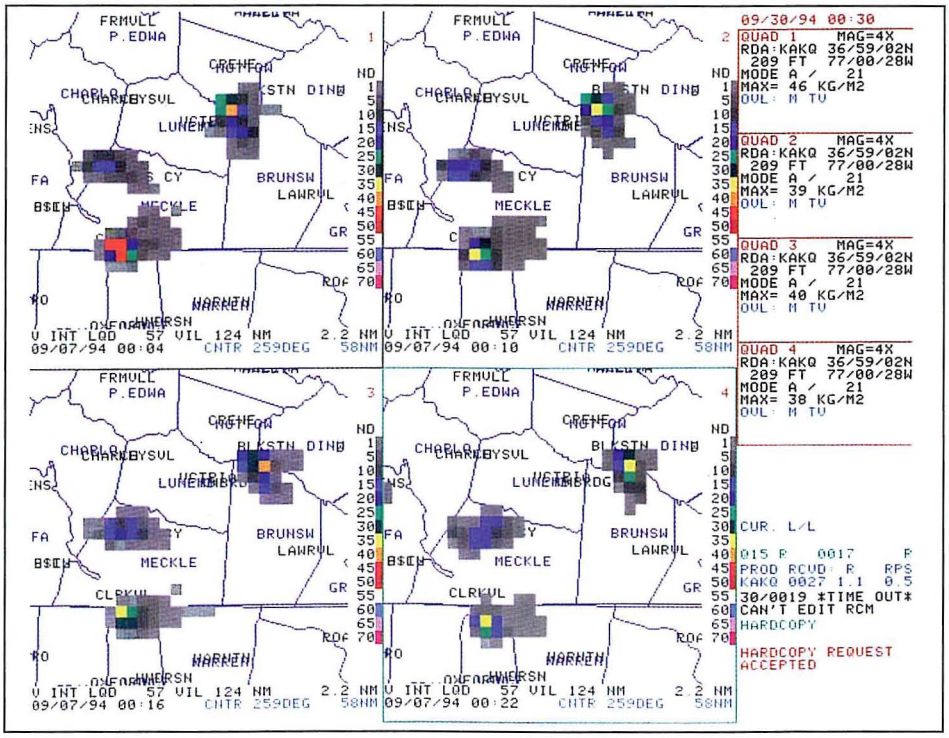

Fig. 9. Same as Fig. 6 except beginning at 0004 UTC 7 September 1994 (upper left). Maximum values of vertically integrated liquid for each volume scan are 46, 39, 40 and 38 for quadrants one, two, three and four, respectively.

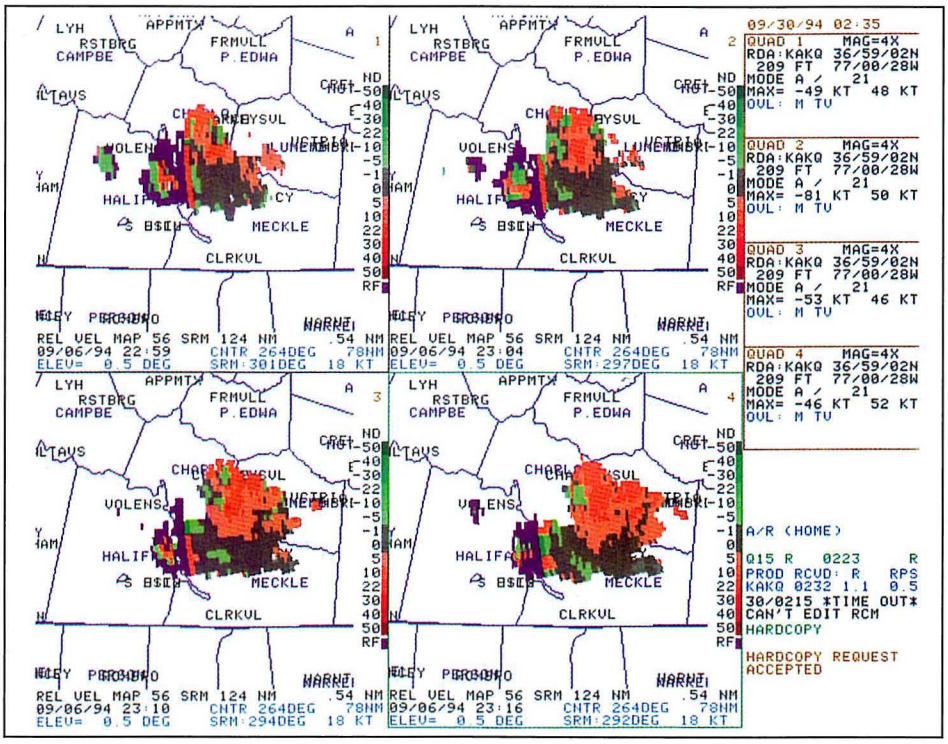

Fig. 10. The Wakefield, Virginia, WSR-88D storm-relative mean radial velocity products beginning at 2259 UTC 6 September 1994 (upper left). The range of coverage is 124 nm (230 km) magnified two times. Resolution is 1° × .54 nm (0.5 km). Storm motion subtracted from base radial velocities was 301°/18 kt (upper left), 297°/18 kt (upper right), 294°/18 kt (lower left), and 292°/18 kt (lower right). The color tables on the right of each quarter panel depict the intervals of velocity in units of knots, and the "RF" denotes range folding. Green colors indicate radial velocities toward the radar, red colors indicate outbound velocities. The maximum inbound and outbound velocities are labeled as negative and positive values, respectively, and are listed to the right of the displayed products. Due to anomalous propagation, these maximum values can be unrepresentative of actual maximum velocities. Maximum inbound and outbound velocities for each quadrant are −49 kt and 48 kt (quadrant 1), −81 kt and 50 kt (quadrant 2), −53 kt and 46 kt (quadrant 3), and −46 kt and 52 kt (quadrant 4).

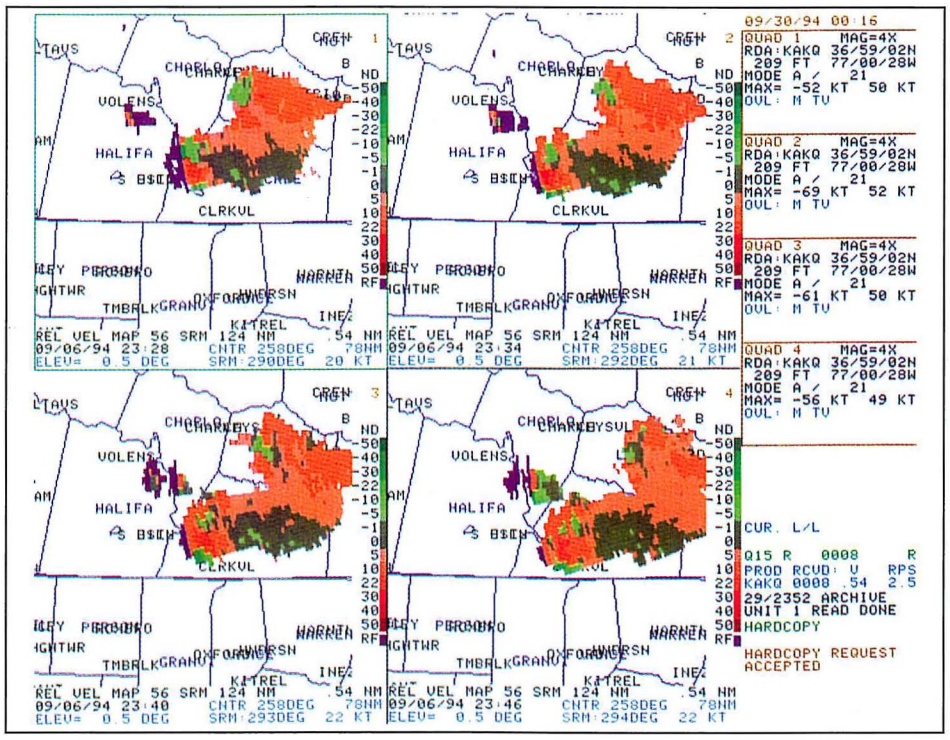

Fig. 11. Same as Fig. 10 except beginning at 2328 UTC 6 September 1994 (upper left). Maximum inbound and outbound velocities for each quadrant are −52 kt and 50 kt (quadrant 1), −69 kt and 52 kt (quadrant 2), −61 kt and 50 kt (quadrant 3), and −56 kt and 49 kt (quadrant 4).

The left-mover exhibited weak anticyclonic low-level rotation in the southern region of the storm within 15 minutes after the split occurred. The peak mean anticyclonic rotational velocity observed in the left-mover was 22 kt between 2234 and 2358 UTC, 45–75 minutes after the split occurred. The anticyclonic rotation observed at the 1.5° elevation angle in the left-mover was of similar magnitude as the magnitude at the 0.5° elevation angle, which was considered to be a very weak anticyclonic mesocyclone at best (the radar does not depict anticyclonic mesocyclones so the operator must make the determination) and too weak for anticyclonic circulations to reach the ground resulting in no anticyclonic tornado activity in the left-mover.

The left-mover also exhibited low-level cyclonic rotation on the northern region of the storm with peak mean rotational velocities of 26 kt average rotation between 2334 and 2346 UTC, 45–55 minutes after the split occurred. The peak cyclonic rotation was stronger than the peak anticyclonic rotation in the left-mover. The inbound velocity signature on the western side of the high-reflectivity core supports the assertion that there were anticyclonic and cyclonic circulations in the left-mover. The center of cyclonic rotation observed at the 1.5° elevation angle was displaced slightly south of the 0.5° elevation angle center of cyclonic rotation resulting in a vertical non-correlation and non-classification as a mesocyclone. Similar to the right-mover, the low-level circulation was too shallow for it to reach the ground resulting in no cyclonic tornado activity associated with the left-mover.

The widespread network of Doppler radars across the United States should provide many opportunities to observe splitting thunderstorms and the resultant left- and right-moving storms. More case studies are needed for a complete understanding of the precursor conditions for the development of splitting cells, as well as recognition of important reflectivity and wind structure characteristics in the thunderstorms (initial and split storms) to provide more advanced warning of the associated severe weather.

Acknowledgments

I would like to thank Hugh Cobb, Science and Operations Officer at NWSO Wakefield, and Bill Sammler, Warning Coordination Meteorologist at NWSO Wakefield as well as the rest of the Wakefield staff for their comments and support during this study. I would also like to thank Steve Kuhl and Gary Carter of the Scientific Services Division at the NWS Eastern Region Headquarters for their valuable input. Finally, I would like to thank Peter Roohr and John Erdman of Colorado State University as well as Rusty Pfost, Science and Operations Officer at NWSFO Jackson, Mississippi for their reviews.

Author

Neil A. Stuart is a forecaster at the National Weather Service Office in Wakefield, Virginia. Primary duties include preparing aviation forecasts, using the Wakefield, Virginia WSR-88D and Dover, Delaware WSR-88D. He also prepares warnings and statements, short term forecasts and provides forecast input to area National Weather Service Forecast Offices. Neil's interests include severe weather, radar interpretation and mesoscale analysis. Neil received his B.S. in Meteorology from the State University Of New York at Albany in 1990.

References

Achtmeier, G. L., 1969: Some observations of splitting thunderstorms over Iowa on August 25–26, 1965. Preprints, *Sixth Conference on Severe Local Storms*, Chicago, Amer. Meteor. Soc., 89–94.

Atlas, David, Ed., 1990: *Radar in Meteorology.* American Meteorological Society, Chapter 15, 118–119.

Brooks, H. E., C. A. Doswell III and J. Cooper, 1994: On the environments of tornadic and nontornadic mesocyclones. *Wea. Forecasting*, 9, 606–618.

Brown, R. A., 1992: Initiation and evolution of updraft rotation within an incipient supercell thunderstorm. *J. Atmos. Sci.*, 49, 1997–2014.

_____, and R. J. Meitín, 1994: Evolution and morphology of two splitting thunderstorms with dominant left-moving members. *Mon. Wea. Rev.*, 122, 2052–2067.

Burgess, D. W., L. R. Lemon, and G. L. Achtmeier, 1976: Severe storm splitting and left-moving storm structure. The Union City Tornado of 24 May, 1973, *NOAA Technical Memorandum* ERL NSSL-80, National Weather Service, U.S. Department of Commerce, 53–66.

_____, R. R. Lee, S. S. Parker and D. L. Floyd, 1995: A study of mini supercells observed by WSR-88D radars. Preprints, *27th Conference on Radar Meteorology*, Vail, Colorado, Amer. Meteor. Soc., 4–6.

Davies-Jones, R. P., D. W. Burgess, and M. Foster, 1990: Test of helicity as a tornado forecast parameter. Preprints, *16th Conference on Severe Local Storms*, Kananaskis Park, Alberta, Canada, Amer. Meteor. Soc., 588–92.

Hart, J. A., and W. D. Korotky, 1991: The SHARP workstation V. 1.50. A Skew T/Hodograph Analysis and Research Program for the IBM and Compatible PC, User's Manual, NOAA/NWS Forecast Office, Charleston, West Virginia.

Hitschfield, W., 1960: The motion and erosion of convective storms in severe vertical wind shear. *J. Meteor.*, 17, 270–282.

Johns, R. H., J. M. Davies, and P. W. Leftwich, 1990: An Examination of the relationship of the 0–2 km AGL "positive" wind shear to potential buoyant energy in strong and violent tornado situations. Preprints, *16th Conference on Severe Local Storms*, Kananaskis Park, Alberta, Canada, Amer. Meteor. Soc., 593–598.

Klazura, G. E., and D. A. Imy, 1993: A description of the initial set of analysis products available from the NEXRAD WSR-88D system. *Bull. Amer. Meteor. Soc.*, 74, 1293–1311.

Kubesh, R. J., D. J. Musil, R. D. Farley, and H. D. Orville, 1988: The 1 August 1981 CCOPE storm: Observations and modeling results. *J. Appl. Meteor.*, 27, 216–243.

Kuhl, S. C., 1994: A preliminary examination of the WSR-88D storm relative velocity map product for tornadic events within the eastern region of the National Weather Service. Postprints, *First WSR-88D User's Conference,* NOAA, U.S. Department of Commerce, 339–350.

Lazarus, S. M. and K. K. Droegemeier, 1990: The influence of helicity on the stability and morphology of numerically simulated storms. Preprints, *16th Conference on Severe Local Storms*, Kananaskis Park, Alberta, Canada, Amer. Meteor. Soc., 269–274.

Miller, R. C., 1972: Notes on Analysis and Severe Storm Forecasting Procedures of the Air Force Global Weather Central. *AWS Tech. Rpt. 200.* (Available from AWS Technical Library, 859 Buchanan Street, Scott AFB, Illinois 62225-5116)

National Weather Service, 1991: Federal Meteorological Handbook Number 11, Part C. NOAA, U.S. Department of Commerce. 3.6, pp. 3.28–3.30, 3.9, pp. 3.34–3.37.

_____, 1994: WSR-88D Operations Course. National Oceanic and Atmospheric Administration, U.S. Dept. of Commerce, National Weather Service. Topic 8, Lesson 3, 30.

Rotunno, R., and J. B. Klemp, 1982: The influence of the shear-induced pressure gradient on thunderstorm motion. *Mon. Wea. Rev.*, 110, 136–151.

Vasiloff, S. V., M. H. Jain, D. L. Keller, A. Witt, V. T. Wood, P. L. Spencer, G. J. Stumpf, and M. D. Elits, 1993: An evaluation of two Doppler radar mesocyclone detection algorithms. Preprints, *26th Int. Conf. on Radar Meteorology*, Norman, Oklahoma, Amer. Meteor. Soc., 657–659.

Weissman, M. L. and J. B. Klemp, 1982: The dependence of numerically simulated convective storms on vertical wind shear and buoyancy. *Mon. Wea. Rev.*, 110, 504–520.

Wilhelmson, R. B., and J. B. Klemp, 1981: A three-dimensional numerical simulation of splitting severe thunderstorms on 3 April 1964. *J. Atmos. Sci.*, 38, 1581–1600.